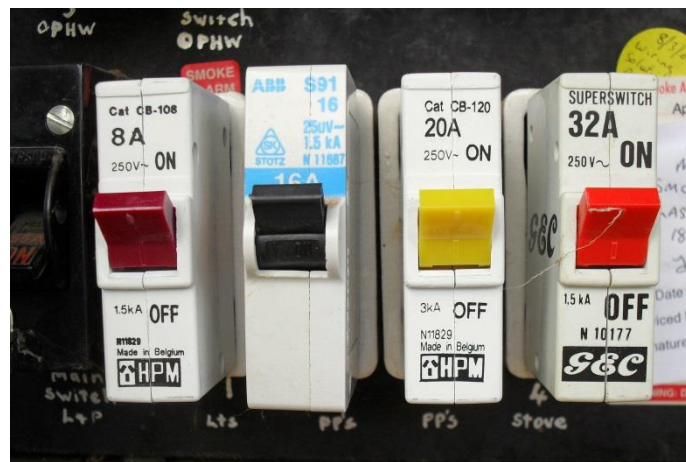


Problem 5

Bimetallic Oscillator

A simple electric oscillator can be made using a bimetallic contact-breaker. Investigate the relevant parameters that affect the frequency of such oscillator.



Structure

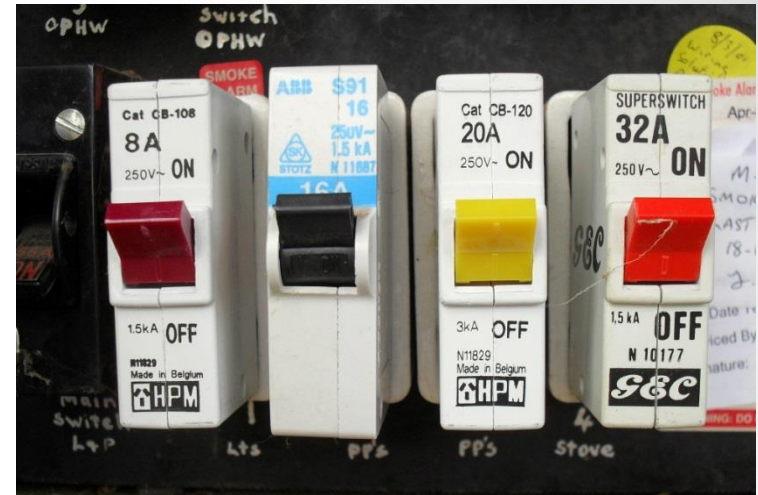
- ❖ General Intro – remember the fuses? origin of the problematics
- ❖ Circuit breakers and MCB typology/characteristics.
- ❖ The construction of an MCB, disassembling an MCB
- ❖ The bimetallic strip, how it works, theory, DIY
- ❖ How to construct a bimetallic “oscillator”
- ❖ Use of ‘snapping action’ bimetallic oscillators in TEH

The sources are quoted on the slides.

Examples – circuit breakers

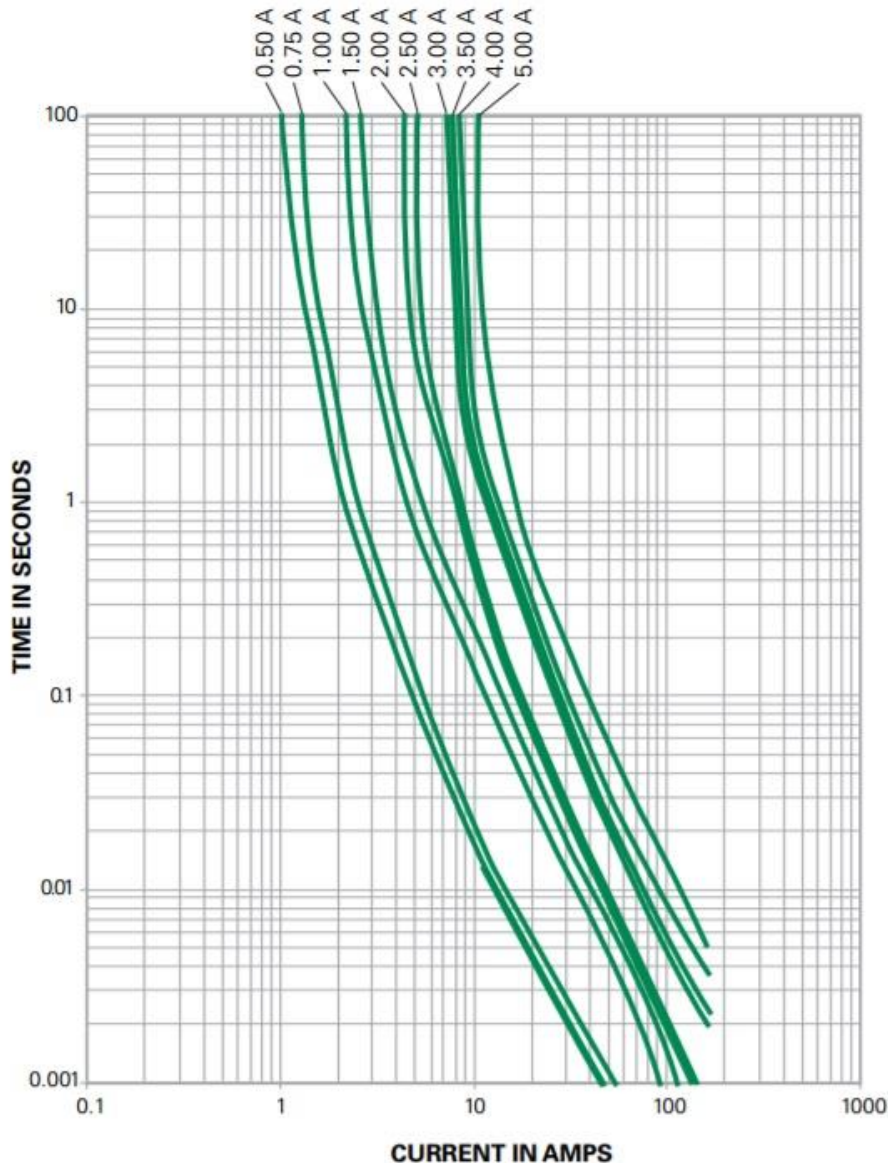


<https://www.electricaltechnology.org/2019/09/fuse-circuit-breaker-symbols.html>



Wright, A., and Newbery, P.G., *Electric Fuses*, 3rd Ed., Institution of Electrical Engineers, Stevenage, UK (2004)

Fuse - Timing



(Show <https://www.ultracal.com/articles/fusingr.pdf> "Fusing Currents in Traces ")

Onderdonck's approx for Cu with $T_{ref}=20^{\circ}\text{C}$, melting at 1083°C

$$t = \left(\frac{1}{33.5} \right) \left[\log_{10} \left(\frac{\Delta T}{234 + T_{ref}} + 1 \right) * \left(\frac{A}{I} \right)^2 \right]$$

$$t = .0346 * (A/I)^2$$

For Fuse Model

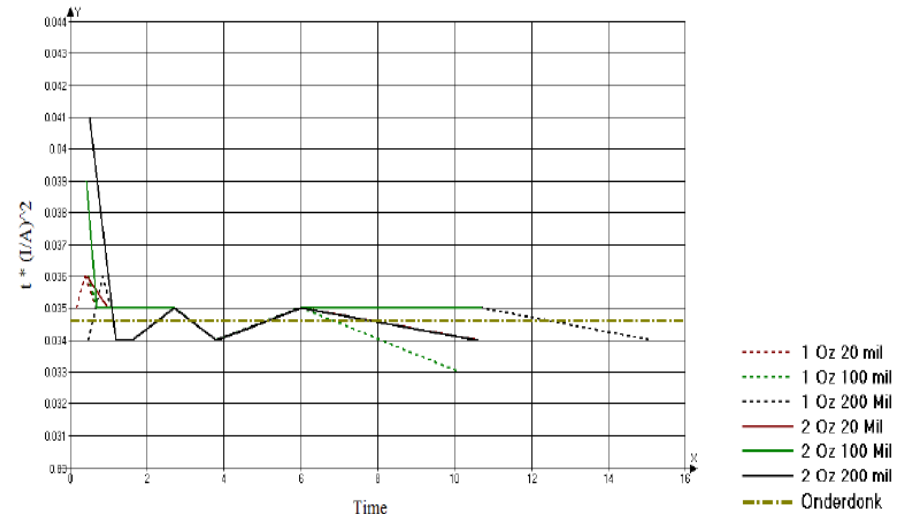


Figure 6

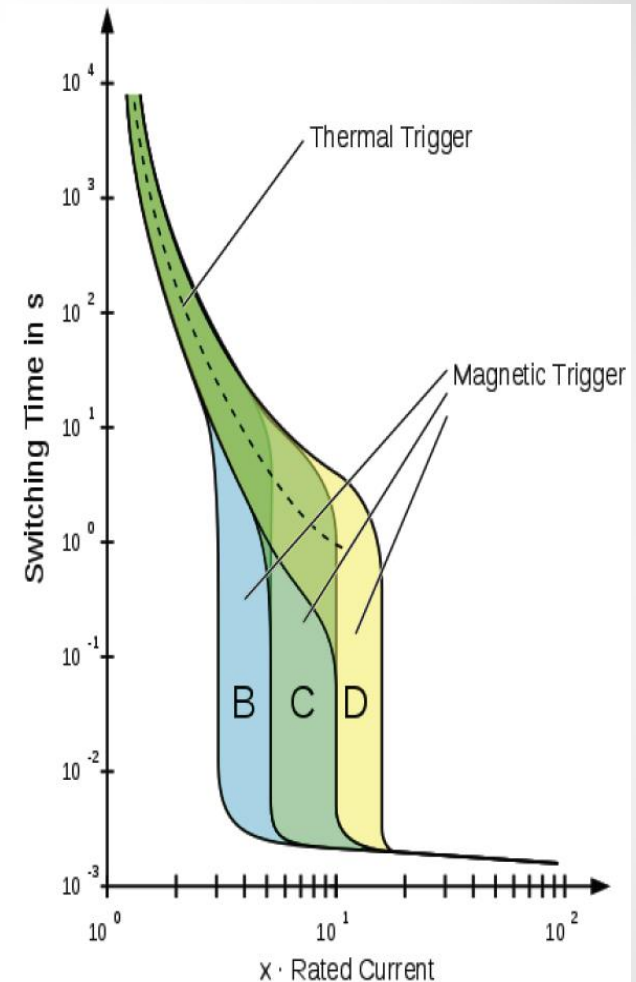
Plot of $t * (I/A)^2$ for the various configuration simulations of the fuse trace.

Examples – circuit breakers

For low voltage distribution circuit breakers, International Standard IEC 60898-1 defines the rated current as the **maximum current that the breaker is designed to carry continuously**.

The commonly available preferred values for the rated current are **1 A, 2 A, 4 A, 6 A, 10 A, 13 A, 16 A, 20 A, 25 A, 32 A, 40 A, 50 A, 63 A, 80 A, 100 A, 125 A**.

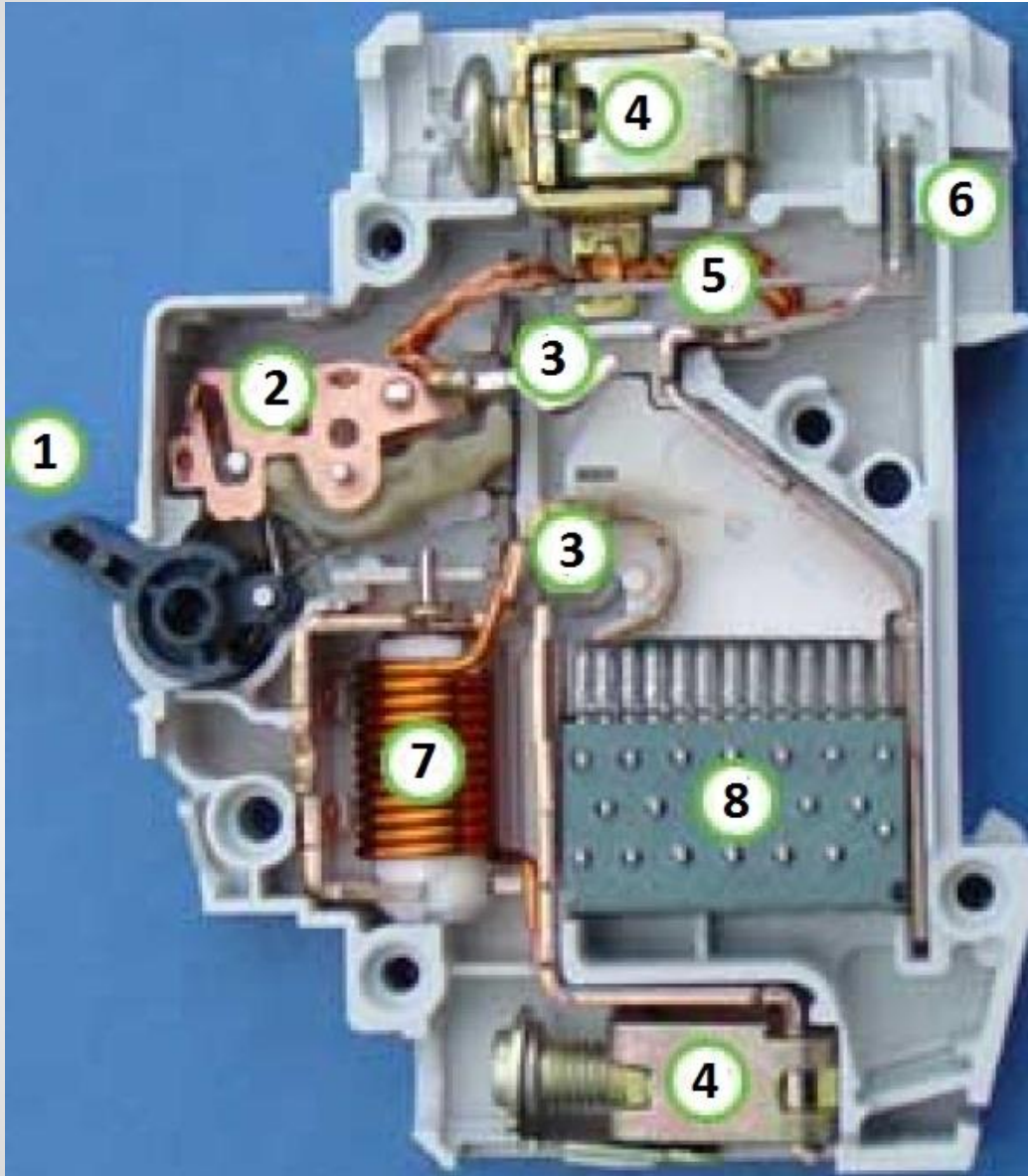
Type	Instantaneous tripping current
B	3-5 times rated current I_n For example a 10 A device will trip at 30–50 A
C	5 to 10 times I_n
D	10-20 times I_n
K	8 to 12 times I_n For the protection of loads that cause frequent short duration (approximately 400 ms to 2 s) current peaks in normal operation.
Z	2 to 3 times I_n for periods in the order of tens of seconds. For the protection of loads such as semiconductor devices or measuring circuits using current transformers.



Time till trip versus current as multiple of nominal current

https://en.wikipedia.org/wiki/Circuit_breaker

The inside of a Miniature Circuit Breaker (MCB) -



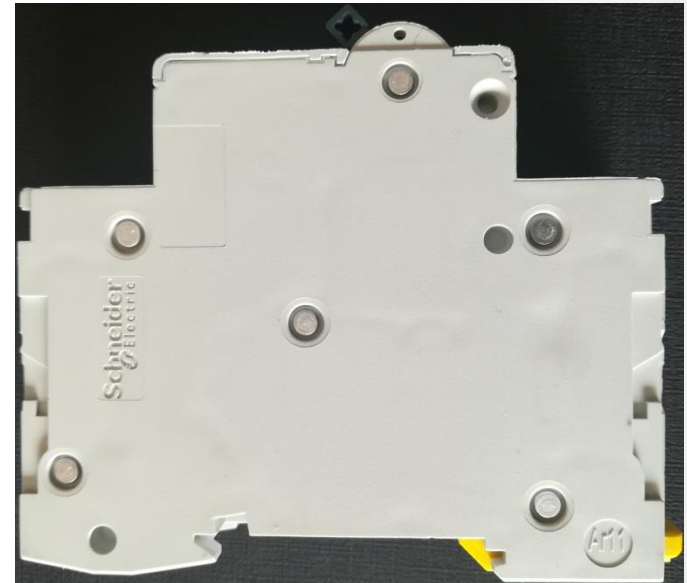
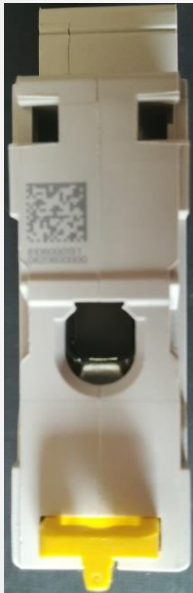
1. **Actuator lever** - used to manually trip and reset the circuit breaker. Also indicates the status of the circuit breaker (On or Off/tripped). Most breakers are designed so they can still trip even if the lever is held or locked in the "on" position. This is sometimes referred to as "free trip" or "positive trip" operation.
2. **Actuator mechanism** - forces the contacts together or apart.
3. **Contacts** - allow current when touching and break the current when moved apart.
4. **Terminals**
5. **Bimetallic strip** - separates contacts in response to smaller, longer-term overcurrents
6. **Calibration screw** - allows the manufacturer to precisely adjust the trip current of the device after assembly.
7. **Solenoid** - separates contacts rapidly in response to high overcurrents
8. **Arc divider/extinguisher**

https://en.wikipedia.org/wiki/Circuit_breaker

Examples – circuit breakers



“MCB” - Miniature Circuit Breaker (up to 125A)
“C6”, rated to interrupt short-circuit
 $I = 6 \text{ kA} = 6000 \text{ A}$ at $230\text{V}\sim$
“C” – 6-10 times the rated current



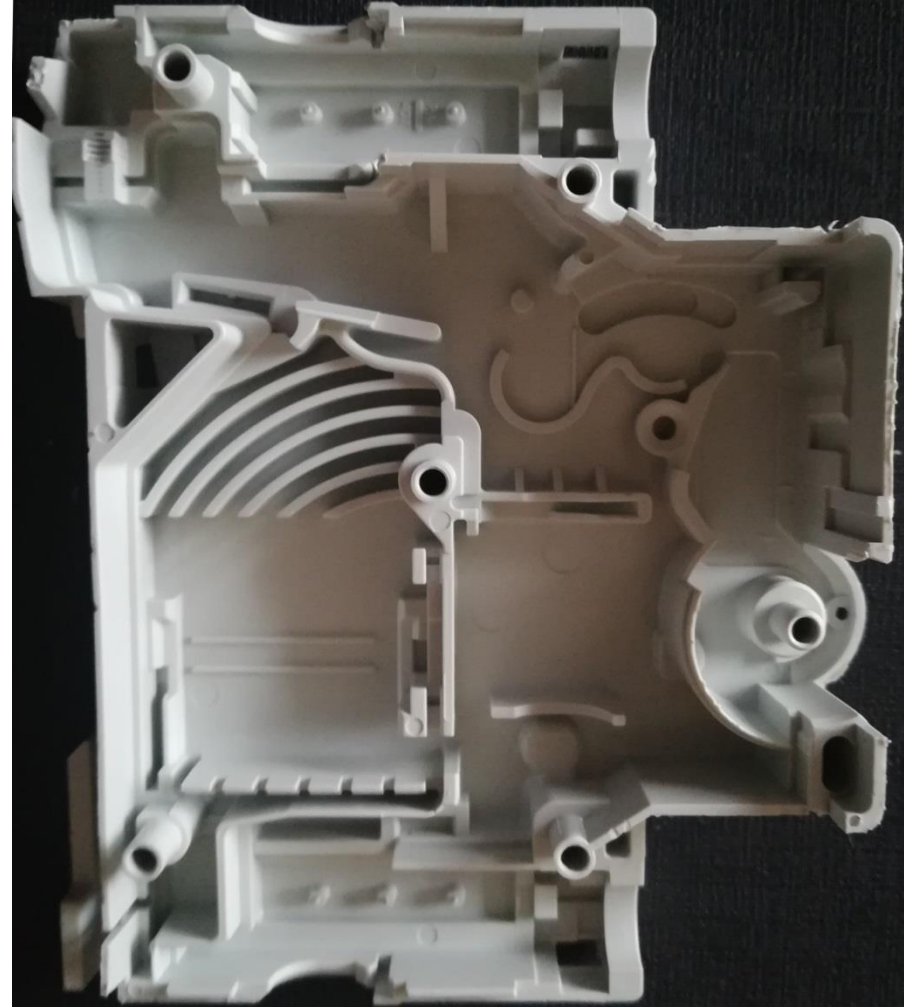
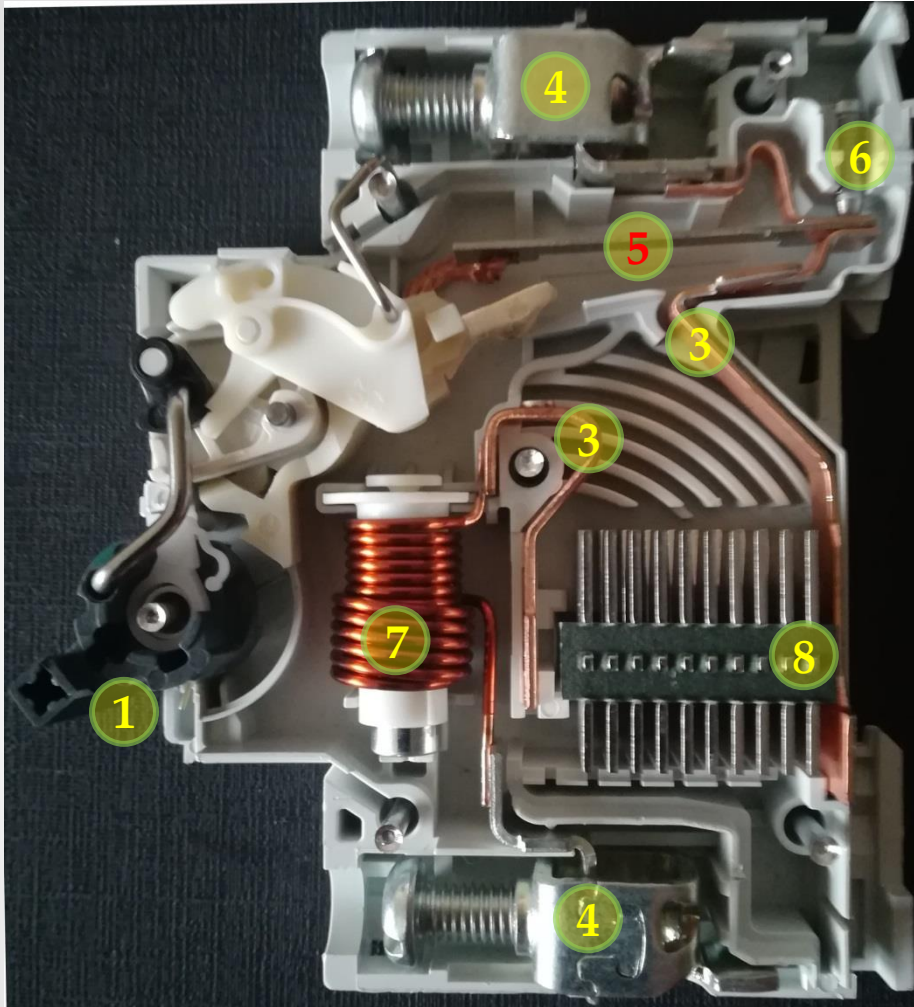
DIN, rail-mounted, “EZ”, “Easy9” by Schneider Electric, *Part.No. EZ9F35106*
Price ~ € 2.30 + tax

The characteristics of low-voltage MCB-s are given in IEC947.

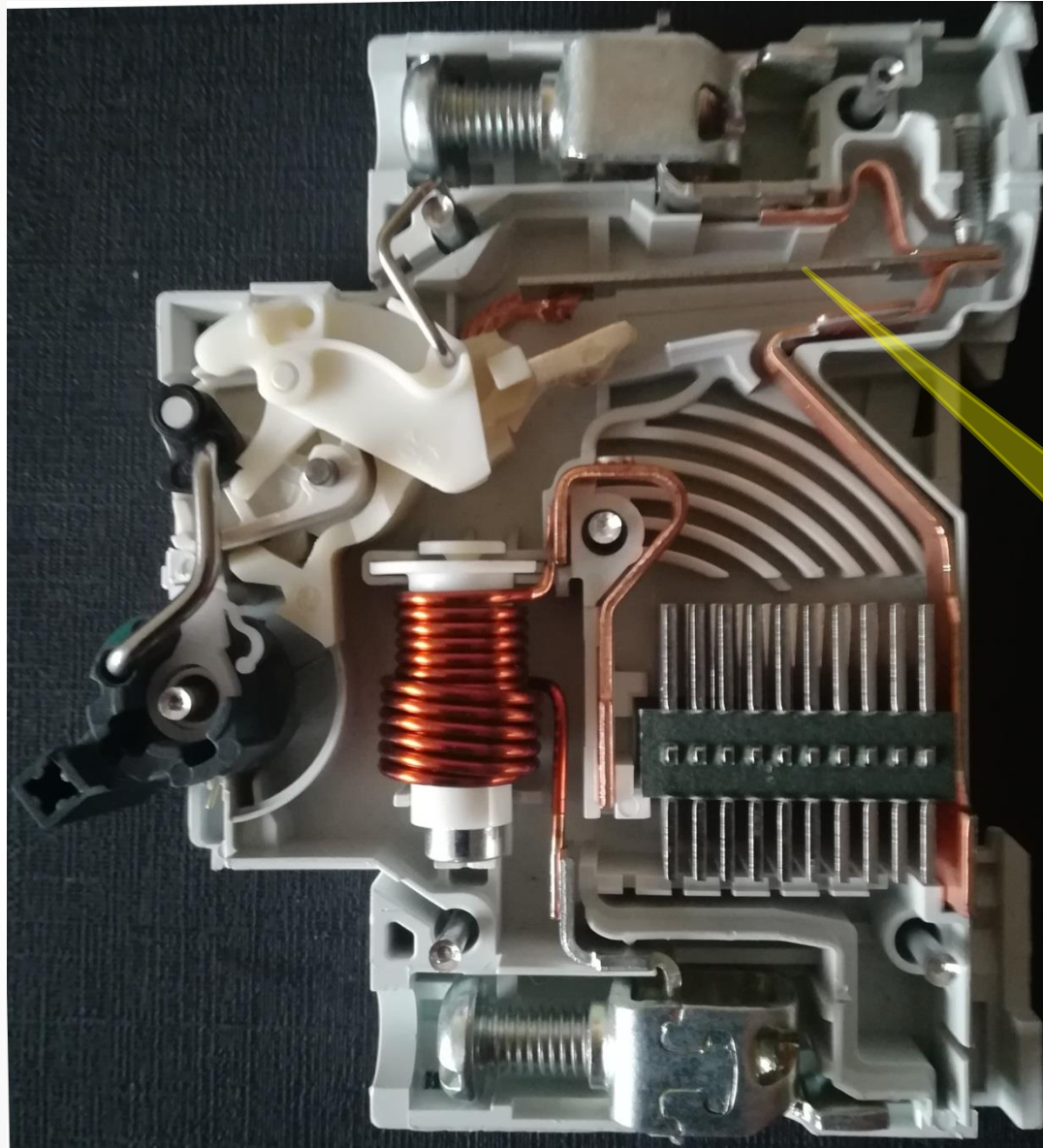
Example MCB – “Easy9” – opening the body



Example MCB (“Easy9”) - disassembly



Example MCB – “Easy9”, inside

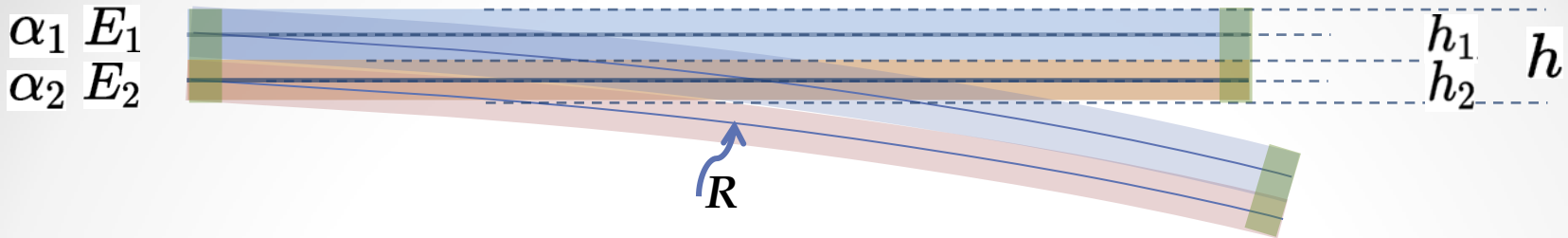


Hot = bent up
Cold = straight

bimetallic
strip

$l = 33 \text{ mm}$

Curvature of a bimetallic strip



The curvature of a bimetallic beam can be described by the following equation:

$$\kappa = \frac{6E_1 E_2 (h_1 + h_2) h_1 h_2 \epsilon}{E_1^2 h_1^4 + 4E_1 E_2 h_1^3 h_2 + 6E_1 E_2 h_1^2 h_2^2 + 4E_1 E_2 h_2^3 h_1 + E_2^2 h_2^4}$$

where $\kappa = 1/R$ and R is the radius of curvature,

E_1 and h_1 are the Young's modulus and height (thickness) of **material one**
 E_2 and h_2 are the Young's modulus and height (thickness) of **material two**.

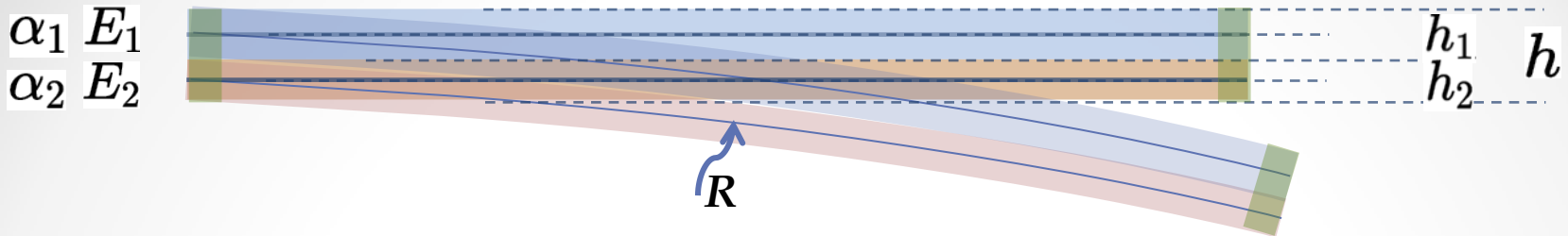
ϵ is the misfit strain, as defined by $\epsilon = (\alpha_1 - \alpha_2) \Delta T$

where α_1 is the coefficient of thermal expansion of **material one** and
 α_2 is the coefficient of thermal expansion of **material two**.

ΔT is the current temperature minus the reference temperature (i.e. the T where the beam has no flexure)

https://en.wikipedia.org/wiki/Bimetallic_strip

Bimetallic strip - some useful approximations



Insight may be gained if the result just given is multiplied on top and bottom by

$$(h_1 + h_2) / E_1 E_2 h_1^2 h_2^2$$

$$\kappa = \frac{6(r_h + 2 + r_h^{-1})}{r_E r_h^2 + 4r_h + 6 + 4r_h^{-1} + r_E^{-1} r_h^{-2}} \frac{\epsilon}{h}$$

where $h = h_1 + h_2$, $r_h = h_1/h_2$ and $r_E = E_1/E_2$.

Since $(1 + x) + (1 + x)^{-1} \approx 2 + O(x^2)$ for small x , which is insensitive to x because of the lack of first order terms, then we may approximate $r_h + r_h^{-1} \approx 2$ for r_h close to unity (and insensitive to r_h), and $r_E r_h^2 + r_E^{-1} r_h^{-2} \approx 2$ for $r_E r_h^2$ close to unity (and insensitive to $r_E r_h^2$).

Thus, unless r_h or r_E are very far from unity we can approximate $\kappa \approx 3\epsilon/2h$

https://en.wikipedia.org/wiki/Bimetallic_strip

Useful materials – Al alloy

Aluminum alloys from drink cans – the body is made of the 3004 alloy (can be drawn easily) and the top is made of the harder 5182 alloy.

3004 Aluminium Alloy Composition by Mass %

<u>Al</u>	<u>Mg</u>	<u>Si</u>	<u>Fe</u>	<u>Cu</u>	<u>Zn</u>	<u>Mn</u>	<u>Remainder</u>
95.6 to 98.2%	0.8 to 1.3%	0.3% max	0.7% max	0.25% max	0.25% max	1.0 to 1.5%	0.15% max



https://en.wikipedia.org/wiki/3004_aluminium_alloy

3004 aluminum is a 3000-series aluminum alloy: the main alloying addition is Mn, and it is formulated for primary forming into wrought products.

3004 is the Aluminum Association (AA) designation for this material.

In European standards, it will be given as EN AW-3004.

AlMn1Mg1 is the EN chemical designation. A93004 is the UNS number.

Additionally, the AFNOR (French) designation is A-M1G

Elastic (Young's, Tensile) Modulus = 70 GPa

Melting Onset-Completion (Solidus to Liquidus) = 630-650 °C

Specific Heat Capacity = 900 J/kg-K

Thermal Conductivity = 160 W/m-K

Thermal Expansion = 24 μm/m-K.

<https://www.makeitfrom.com/material-properties/3004-AlMn1Mg1-3.0526-A93004-Aluminum>

Other useful materials – e.g. steel from cans, etc

Material	Material type	Linear coefficient CLTE α at 20 °C ($\times 10^{-6} \text{ K}^{-1}$)	Volumetric coefficient α_V at 20 °C ($\times 10^{-6} \text{ K}^{-1}$)
<u>Aluminium</u>	Metal	23.1	69
<u>Brass</u>	Metal alloy	19	57
<u>Carbon steel</u>	Metal alloy	10.8	32.4
<u>CFRP</u>		-0.8 ^[15]	Anisotropic
<u>Concrete</u>	Aggregate	12	36
<u>Copper</u>	Metal	17	51
<u>Diamond</u>	Nonmetal	1	3
<u>Ethanol</u>	Liquid	250	750 ^[16]
<u>Gasoline</u>	Liquid	317	950 ^[14]
<u>Glass</u>	Glass	8.5	25.5
<u>Borosilicate glass</u> ^[17]	Glass	3.3 ^[18]	9.9
<u>Glycerine</u>	Liquid		485 ^[17]
<u>Gold</u>	Metal	14	42
<u>Ice</u>	Nonmetal	51	
<u>Invar</u>		1.2	3.6
<u>Iron</u>	Metal	11.8	35.4
<u>Kapton</u>		20 ^[19]	60
<u>Lead</u>	Metal	29	87
<u>Macor</u>		9.3 ^[20]	
<u>Nickel</u>	Metal	13	39

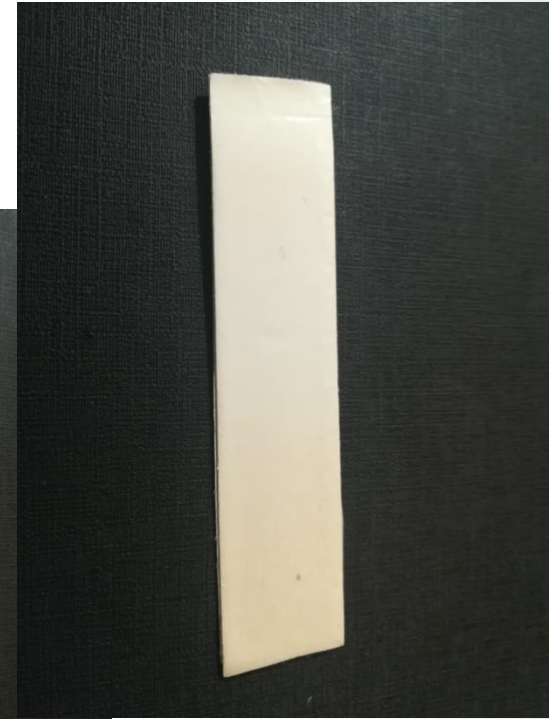
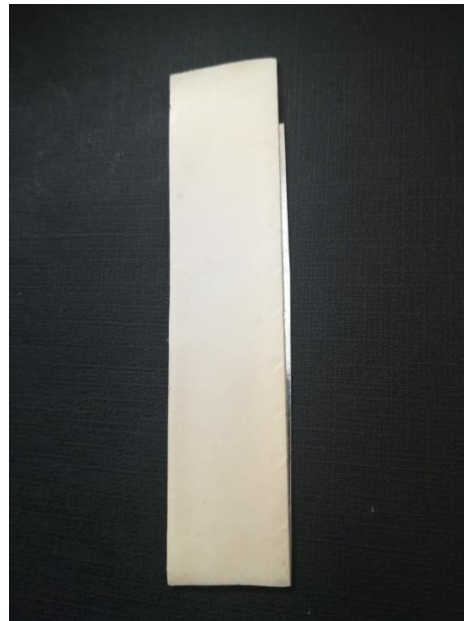


Plate steel used in the canning industry.
Very easy to cut to shape using scissors.

<u>Silver</u>	Metal	18 ^[27]	54
" <u>Sitall</u> "	Glass-ceramic	0±0.15 ^[28]	0±0.45
<u>Stainless steel</u>	Metal alloy	10.1 ~ 17.3	30.3 ~ 51.9
<u>Steel</u>	Metal alloy	11.0 ~ 13.0	33.0 ~ 39.0
<u>Titanium</u>	Metal	8.6	26 ^[29]
<u>Tungsten</u>	Metal	4.5	13.5
<u>Water</u>	Nonmetal	69	207 ^[30]
" <u>Zerodur</u> "	Glass-ceramic	≈0.007-0.1 ^[31]	
ALLVAR Alloy 30	Metal alloy	-30 ^[32]	anisotropic

https://en.wikipedia.org/wiki/Thermal_expansion#Coefficient_of_thermal_expansion

Bimetallic strips and how they are made



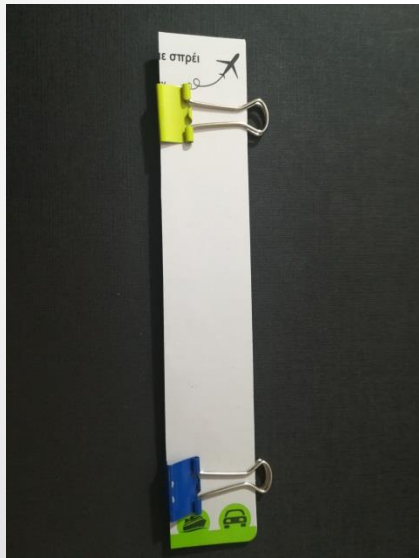
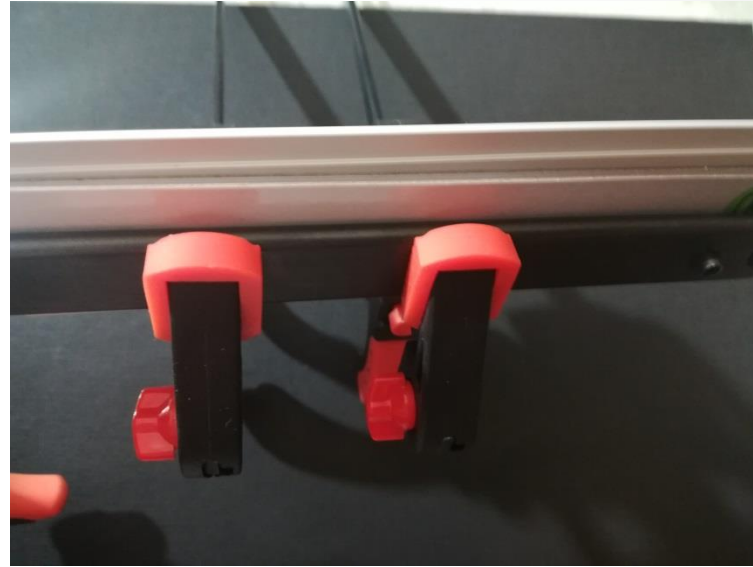
<https://www.electricaltechnology.org/2019/09/fuse-circuit-breaker-symbols.html>

Bimetallic strips and how they are made



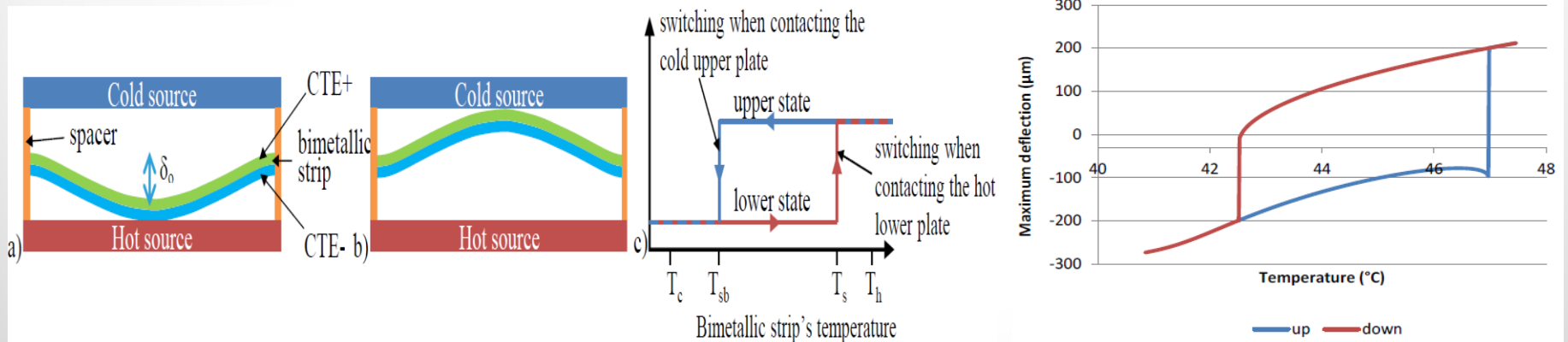
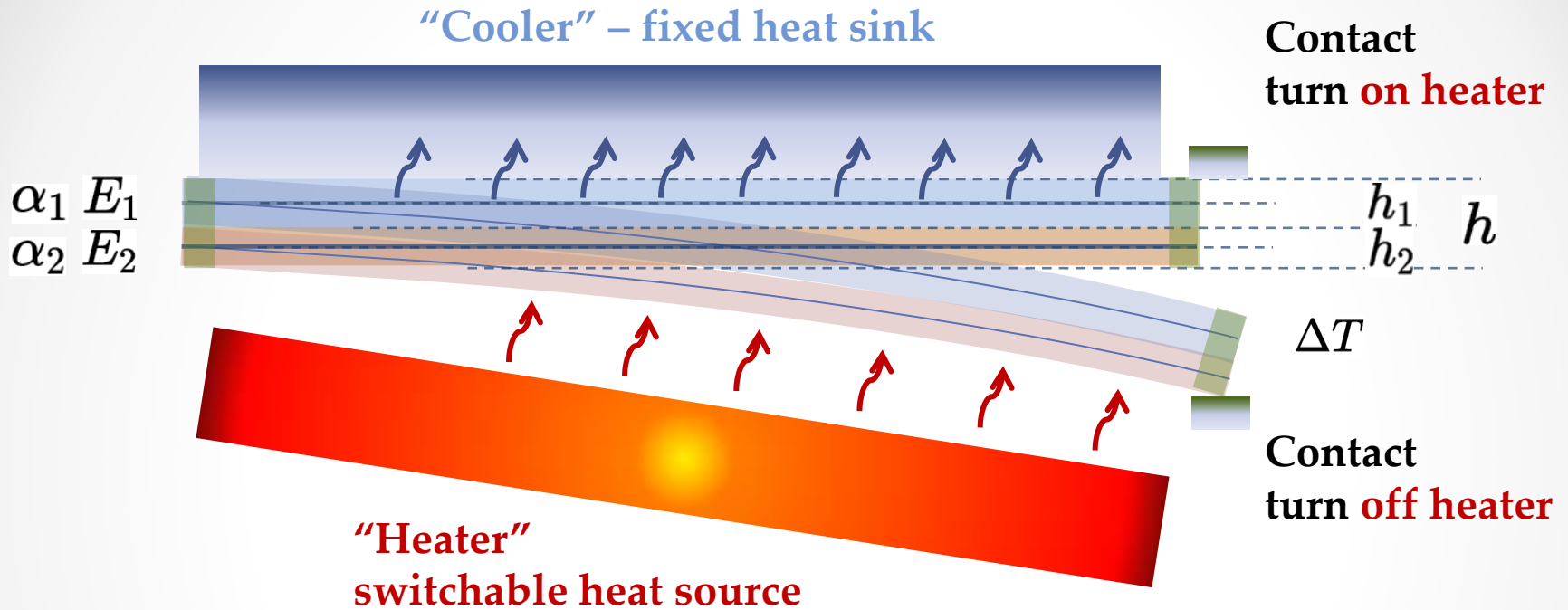
<https://www.electricaltechnology.org/2019/09/fuse-circuit-breaker-symbols.html>

Bimetallic strips and how they are made

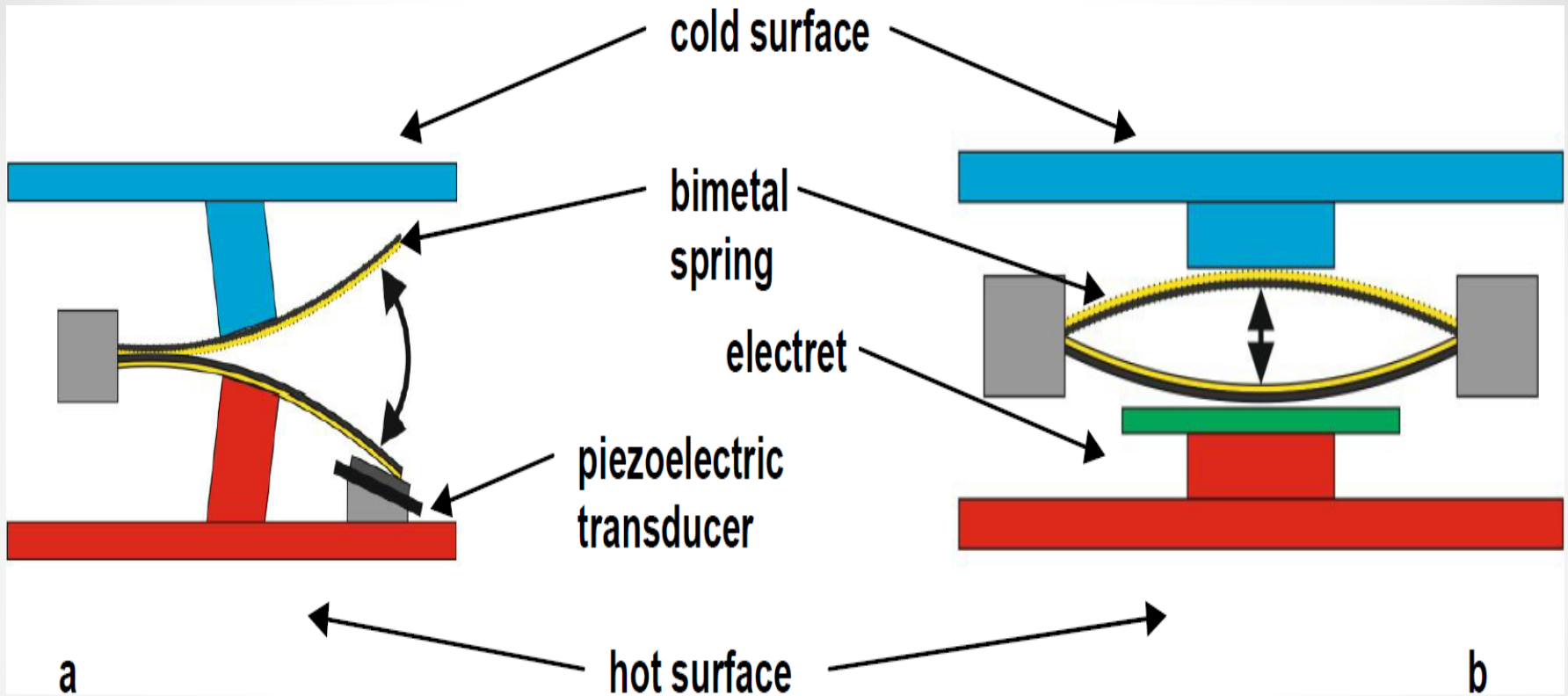


<https://www.electricaltechnology.org/2019/09/fuse-circuit-breaker-symbols.html>

What is a bimetallic 'oscillator'?



Bimetal-based thermal energy harvesting (b-TEH)



P. Prokaryn, *et al.*, 13th Int.Sci.Conf. Optical Sensors & Electronic Sensors, ed. J.Golebiowski, R.Gozdur, Proc. of SPIE, 9291, 92910E

Piezoelectric and electrostatic bimetal-based thermal energy harvesters

A. Arnaud^{1,3}, S. Boisseau², S. Monfray¹, O. Puscasu¹, G. Despesse², J. Boughaleb¹, Y. Sanchez¹, F. Battegay¹, M. Fourel¹, S. Audran¹, F. Boeuf¹, J. Delamare³, G. Delepierre⁴, G. Pitone⁴, T. Skotnicki¹

¹ ST Microelectronics, 850 rue J. Monnet - 38926 Crolles, France

² CEA, Leti, Minatec Campus, 17 rue des Martyrs - 38054 Grenoble Cedex 9, France

³ G2ELab Grenoble, 25 av. des Martyrs - 38042 Grenoble Cedex 9, France

⁴ Delta Concept, 6 rue de Chamechaude, ZI de l'argentière – 38360 Sassenage, France

E-mail: arthur.arnaud@st.com

Abstract. This paper reports on innovative thermal energy harvesters (TEH) turning heat fluxes into electricity in a two-step conversion, involving (i) a curved bimetallic strip converting thermal gradients into mechanical oscillations, which are then (ii) converted into electricity by a piezoelectric or an electret-based electrostatic transducer. This work mainly focuses on (i) the optimizations of the piezoelectric devices, (ii) a first demonstration of a Wireless Sensor Node powered by our electrostatic transducers, validating the viability of bimetal-based thermal energy harvesters, and (iii) the possibility of future scaled scavengers by a micrometric silicon approach to improve efficiencies and power densities.

<https://iopscience.iop.org/article/10.1088/1742-6596/476/1/012062/pdf>

Bimetal-based thermal energy harvesting (b-TEH)

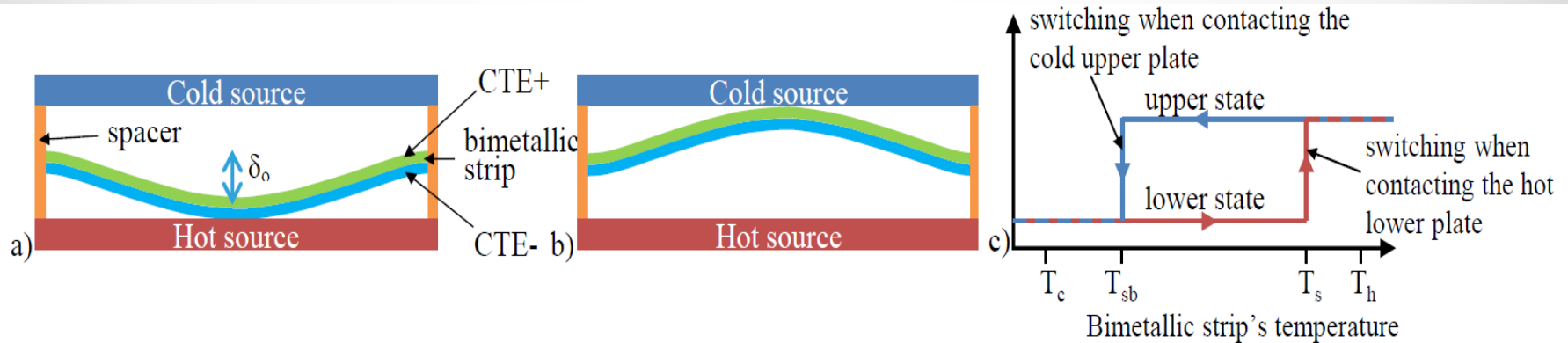


Figure 1. Curved bimetallic strip in a cavity subjected to a thermal gradient (a) lower state and (b) upper state; and (c) hysteresis cycle of the bimetallic strip enabling the oscillations

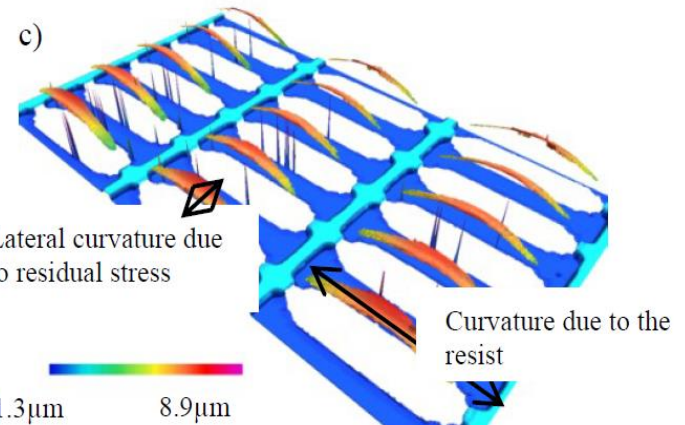
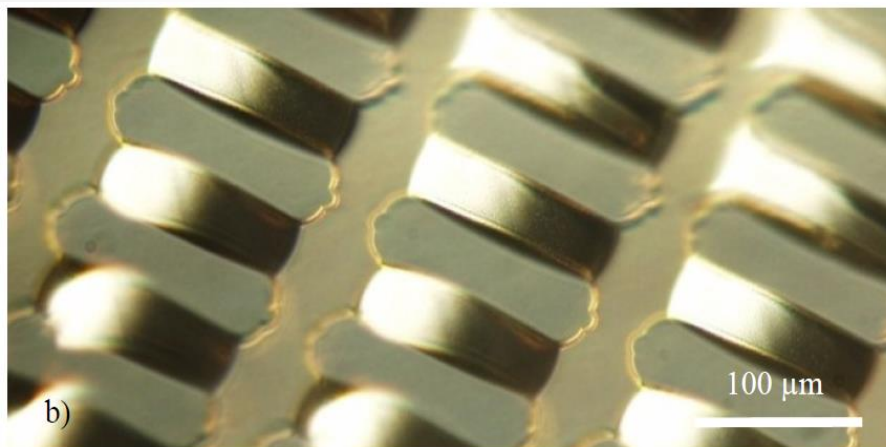


Figure 6. (a) Micro-bimetallic strips process steps (b) Images of Ti-Au bimetallic strips obtained thanks to the new process. (c) Interferometry measurement of the 210 μm -long Ti-Au bimetallic strips curvature at 70 $^\circ\text{C}$.

A. Arnaud, *et al.*, *J. Phys. Conf. Series* **476** (2013) 012062

Bimetal-based thermal energy harvesting (b-TEH)

Thermal energy harvesters with piezoelectric or electrostatic transducer

Piotr Prokaryn^{*a}, Krzysztof Domański^a, Michał Marchewka^a, Daniel Tomaszewski^a, Piotr Grabiec^a,
Onoriu Puscasu^b, Stéphane Monfray^b, Thomas Skotnicki^b

^aInstitute of Electron Technology, Division of Silicon Microsystem and Nanostructure Technology,
Al. Lotników 32/46, 02-668 Warsaw, Poland; ^bST Microelectronics (Crolles 2) SAS, 850 Jean
Monnet st., 38926, Crolles Cedex, France

* prokaryn@ite.waw.pl

ABSTRACT

This paper describes the idea of the energy harvester which converts thermal gradient present in environment into electricity. Two kinds of such devices are proposed and their prototypes are shown and discussed. The main parts of harvesters are bimetallic spring, piezoelectric transducer or electrostatic transducer with electret. The applied piezo-membrane was commercial available product but electrets was made by authors. In the paper a fabrication procedure of electrets formed by the corona discharge process is described. Devices were compared in terms of generated power, charging current, and the voltage across a storage capacitor.

Keywords: energy harvesting, piezoelectric transducers, electrets, bimetals, corona charging

13th International Scientific Conference on Optical Sensors and Electronic Sensors, ed. by J. Golebiowski, R. Gozdur,
Proceedings of SPIE Vol. 9291, 92910E · © 2014 SPIE, CCC code: 0277-786X/14/\$18 · doi: 10.1117/12.2070512

From: <http://proceedings.spiedigitallibrary.org/> Terms of Use: <http://spiedl.org/terms>

Bimetal-based thermal energy harvesting (b-TEH)

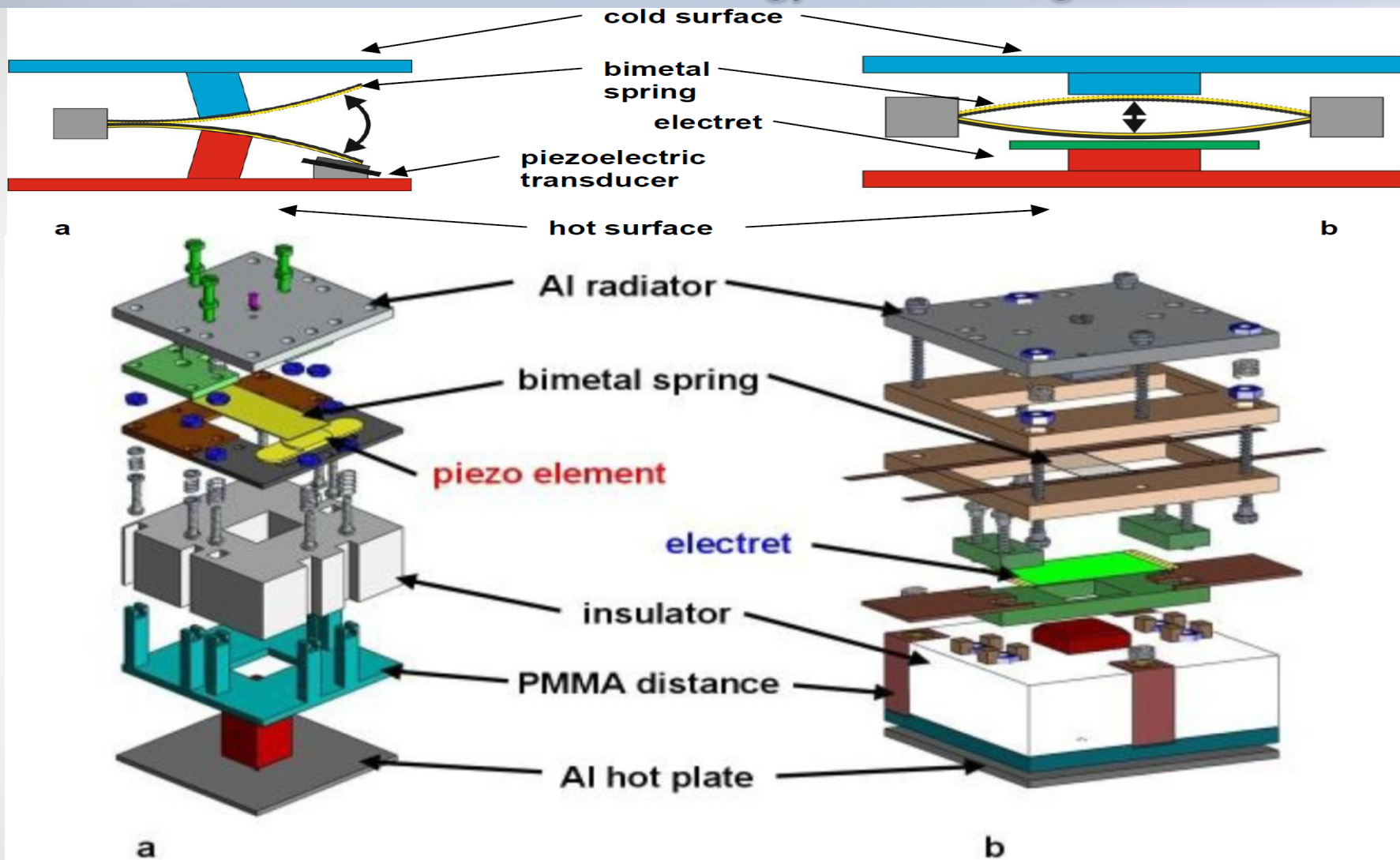
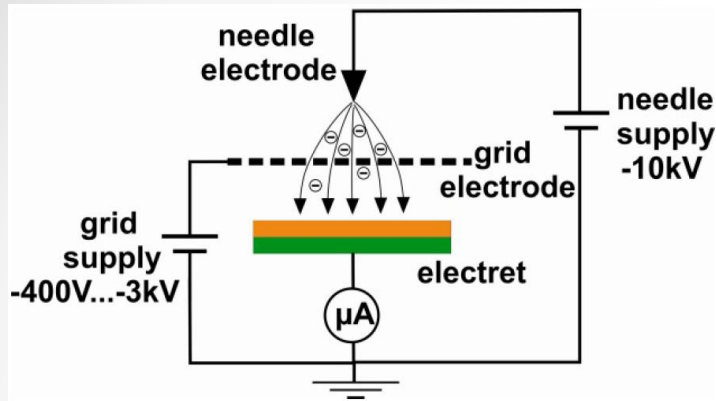


Figure 1. Construction of energy harvesters: a – with piezoelectric transducer; b – with electrostatic transducer

P. Prokaryn, *et al.*, 13th Int. Sci. Conf. Optical Sensors & Electronic Sensors, ed. J. Golebiowski, R. Gozdur, Proc. of SPIE, 9291, 92910E

Making electrets for be-TEH - examples



Making electrets for electrostatic- based harvesting

A corona charging setup with a 3-electrode system:

- needle corona electrode
- grid electrode
- grounded planar electrode w/ electret in its center

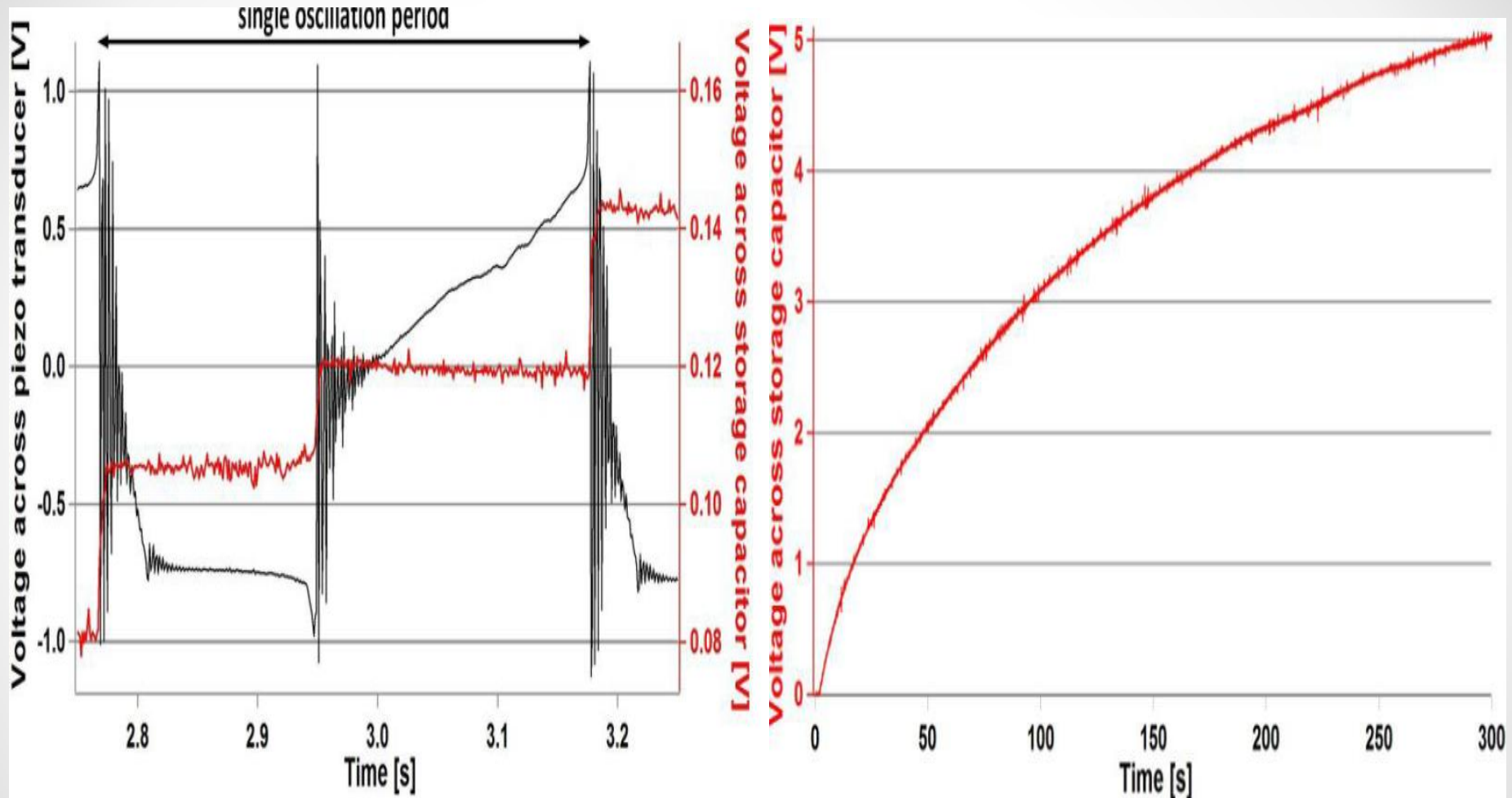
Three types of electrets were fabricated and tested: a 25 μm thick Teflon layer (DuPont™ FEP A100 or PFA LP100) on copper foil, a 15 μm thick polymer CYTOP EGG-811 (commercially available) on copper foil or silicon substrate, and silicon dioxide thermally grown on silicon substrate. The electret samples were corona-charged from a high-voltage needle electrode at constant voltage of -10 kV (or +10 kV) at standard atmospheric conditions (Fig. 3). The surface potential of charged dielectric films was measured using electrostatic voltmeter Trek 347 and end-viewing probe mounted on a 3D micromanipulator, which allowed for positioning of the probe along each axis with a precision of 0.1 mm. The effective surface charge density σ was calculated according the formula: $\sigma = \epsilon_r \epsilon_0 V_z / d$, where ϵ_r is the relative permittivity of an electret material, ϵ_0 is the permittivity of vacuum, V_z is the measured surface potential, and d is the thickness of electret layer. The highest value of the surface charge density, exceeding 10 mC/m², was achieved for SiO₂/Si₃N₄ samples. The densities of electric charge accumulated in the CYTOP or Teflon layers were at least a few times lower. Thus only the harvester with SiO₂ electret was compared with the piezoelectric device as described in more detail below.

The silicon oxide electret samples were manufactured using 4-inch boron doped silicon wafers of (100) crystal orientation and 6 – 10 Ωcm resistivity. The SiO₂ layer (350 nm, 500 nm or 10000 nm thick) was thermally grown at 1150 °C in dry oxidation process. After standard photolithography process, the top SiO₂ layer was etched to define dicing streets. Silicon dioxide was covered with 65 nm thick Si₃N₄ layer deposited in LPCVD process. The dielectric layers were etched off from the backside of the wafers and 700 nm thick Al layer was sputtered on the backsides. The wafers were cut into 14 mm x 35 mm samples, which were annealed for two hours at 150 °C just before the charging process. Some samples were additionally coated on the front side with HMDS (hexamethyldisilazane) layer or acrylic layer and heated on hotplate at 100 °C for 15 minutes. Electrets were charged in corona discharge process at room or elevated temperature (100-200 °C) using a tip and grid electrodes with maximum voltage of 10 kV applied to the tip and 400 V or 500 V applied to the grid [5-6]. Both negatively and positively charged electrets were successfully fabricated with this method.

P. Prokaryn, *et al.*, 13th Int.Sci.Conf. Optical Sensors & Electronic Sensors, ed. J.Golebiowski, R.Gozdur, Proc. of SPIE, [9291](#), 92910E

b-TEH – charging a storage capacitor

Charging of 80 μF storage capacitor using the harvester with piezoelectric converter/transducer

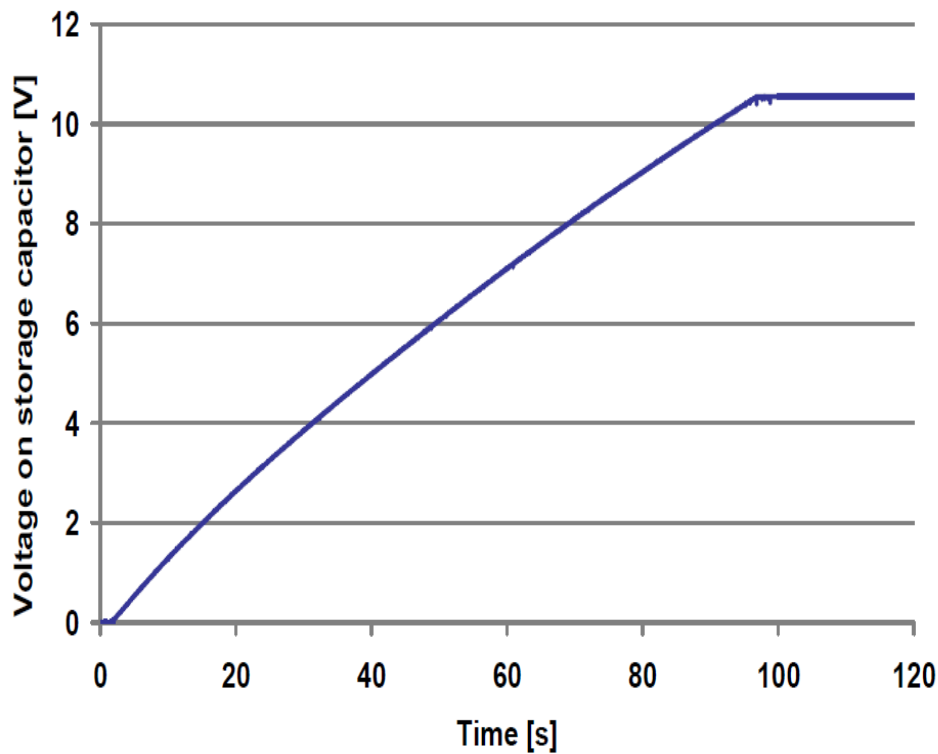


Black: voltage pulses across the piezoelectric
Red: increase of voltage across storage capacitor

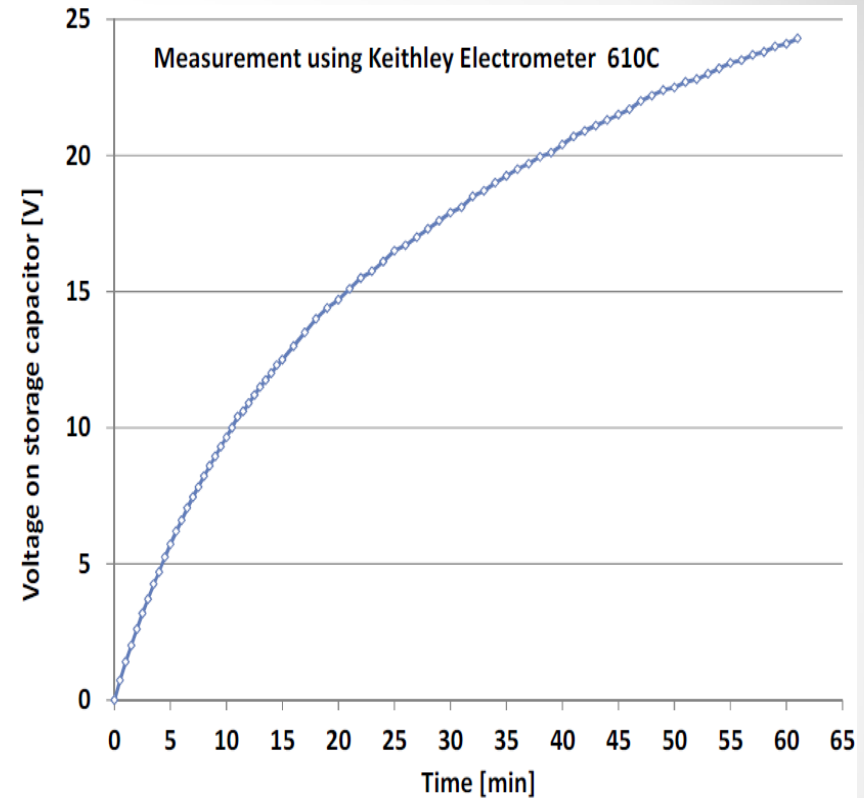
300 s charging process, measured with a DAQ

P. Prokaryn, *et al.*, 13th Int.Sci.Conf. Optical Sensors & Electronic Sensors, ed. J.Golebiowski, R.Gozdur, Proc. of SPIE, 9291, 92910E

Bimetal-based thermal energy harvesting (be-TEH)



a



b

Fig. 6 Charging of capacitor using harvester with bimetallic spring oscillating over SiO_2 electret coated with acrylic resin: a. Measurement performed with NI USB 6363 DAQ (constant voltage on a storage capacitor above 10.5 V results from exceeding the measurement range of the DAQ), b. Measurement performed with Keithley electrometer 610C.

Bimetal-based thermal energy harvesting (b-TEH)

2.2. Piezoelectric transducer mechanical optimization

The transducer global efficiency is mainly linked to the quality of the kinetic energy transfer between the bimetallic strip and the transducer, and to the conversion efficiency of the transducer strain energy into electric energy. During this conversion, the energy is either harvested or lost in the clamps. We have focused here on optimizing the piezoelectric transducer to limit the energy losses in the structure.

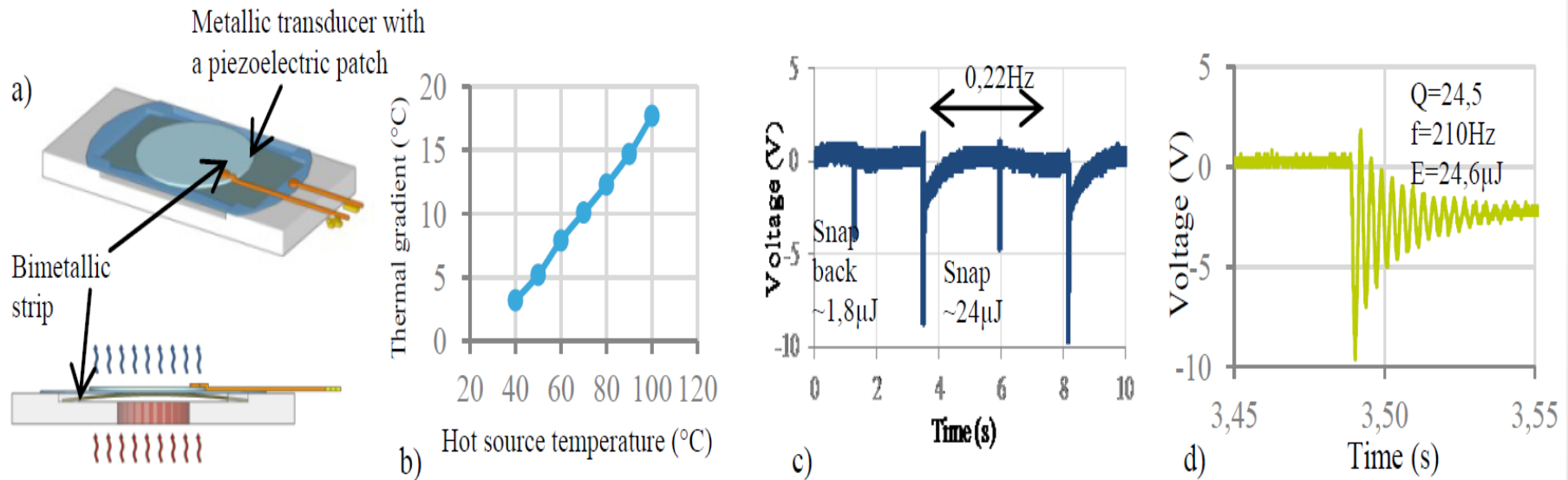


Figure 2. (a) Piezoelectric device principle. (b) Thermal optimization of the device. (c) Output signal of the transducer. (d) Detail of the signal after a bimetallic strip snap

about $5\mu\text{W}$ at 0.22Hz

Bimetal&electret-based thermal energy harvesting (be-TEH)

3. Electrostatic devices

Electret-based electrostatic converters are built on a capacitive architecture made of two plates separated by an air gap and polarized by an electret (figure 3a) [3]. The electret is a permanently charged dielectric that induces charges on the two plates, with $Q_i = Q_1 + Q_2$, where Q_i , Q_1 and Q_2 are respectively, the charges on the electret, the lower electrode and the upper electrode; its equivalent electric model is presented in figure 3b. A relative movement between the two plates induces a new repartition of charges between the two electrodes, converting the mechanical movement into electric charges that are collected by a load (R).

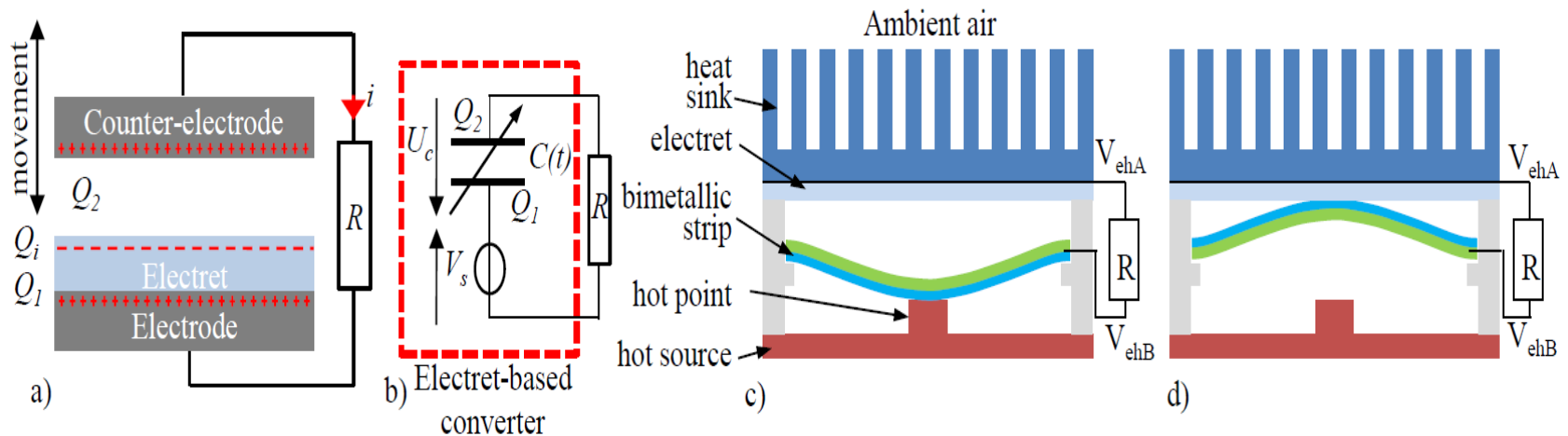


Figure 3. (a) Electret-based converter, (b) equivalent electric model of the electret-based converter, be-TEH in (c) its lower state and (d) its upper plate.

Bimetal&electret-based thermal energy harvesting (be-TEH)

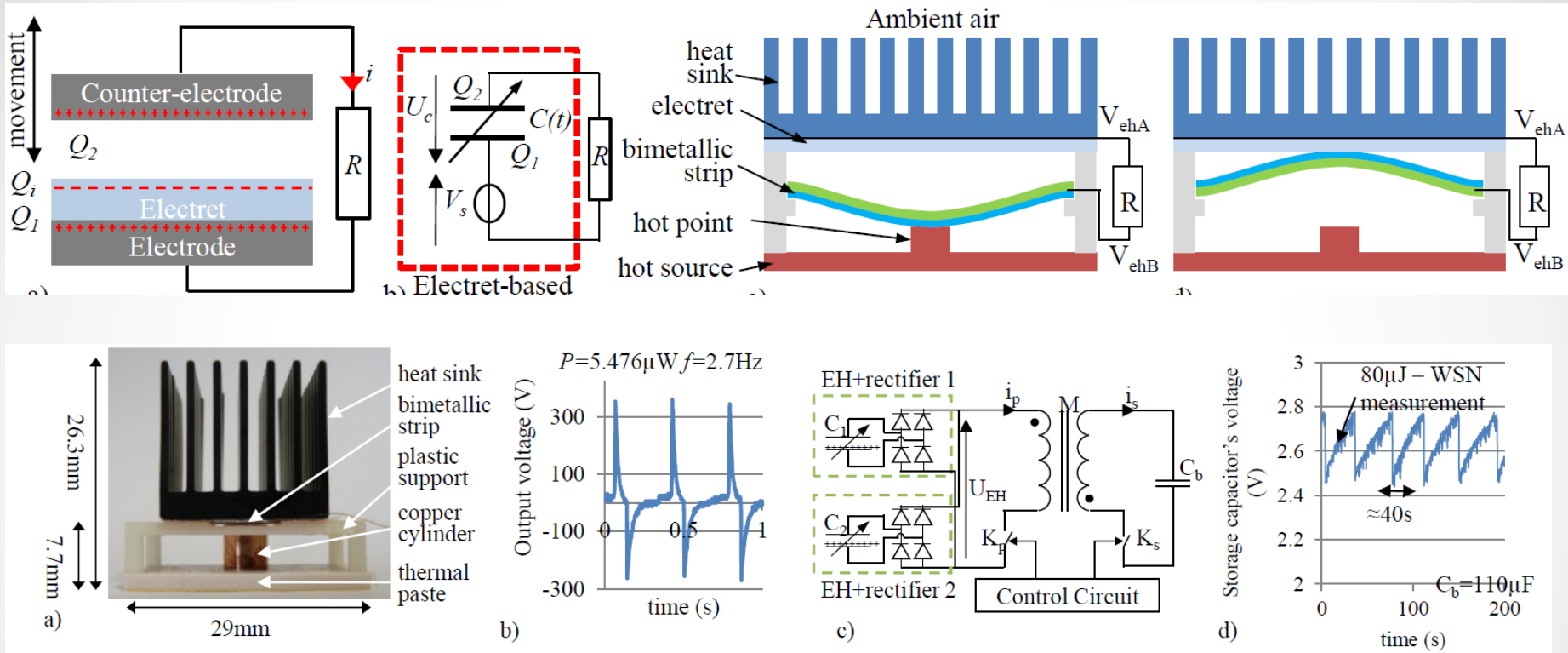


Figure 4. (a) prototype, (b) output voltage (c) power management circuit implementing SECE and (d) WSN supplied by 10 devices in parallel

$5\mu\text{W}$ at 2Hz

Bimetal&electret-based thermal energy harvesting (be-TEH)

As the energy harvester's output voltage is not compatible with standard electronic circuits, a power management circuit implementing SECE (Synchronous Electric Charge Extraction [5]) and withstanding devices in parallel has been manufactured (figure 4c). Ten bimetallic strips have been connected to this power management circuit to power a wireless sensor node consuming $80\mu\text{J}$ per emission every 40 seconds (figure 4d), definitely validating the suitability of be-TEH to power WSN from ambient thermal energy [6].

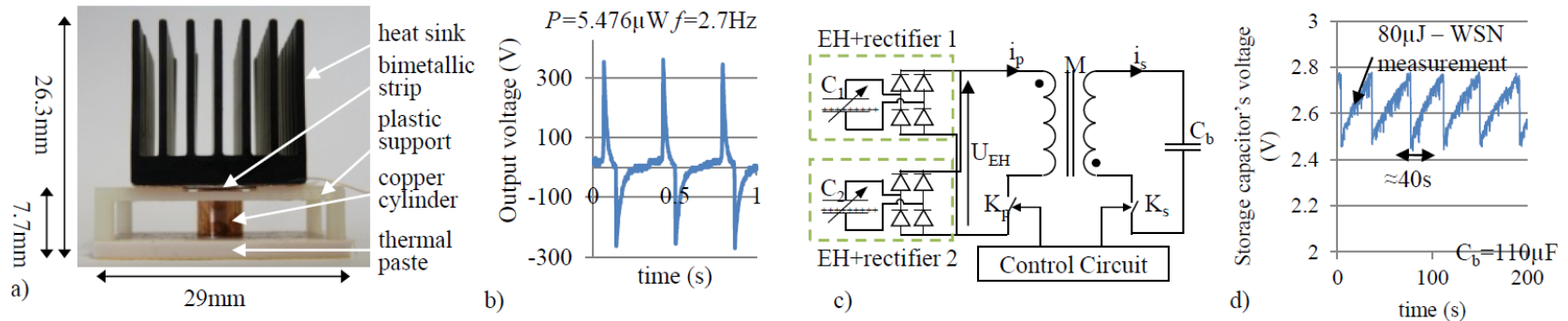


Figure 4. (a) prototype, (b) output voltage (c) power management circuit implementing SECE and (d) WSN supplied by 10 devices in parallel

A. Arnaud, *et al.*, J. Phys. Conf. Series **476** (2013) 012062

Bimetallic strips – mechanical stability and snapping

4. Miniaturization of electrostatic devices

4.1. Bimetallic strips modeling

Timoshenko S, Gere J, Theory of elastic stability, McGraw-Hill, NY, 1961, p.312

As demonstrated by Timoshenko in [9], if its initial curvature δ_0 (see figure 1a) exceeds a critical ratio such that $\delta_0 > t/\sqrt{3}$ (t : total beam thickness), the bimetallic strip will have a snap action. Otherwise, if it is lower, the snap action disappears and the bimetallic strip only buckles slowly. Thanks to this model, the evolution of snapping and snapping-back temperatures for all the different parameters of the bimetallic strips can be plotted in order to evaluate the best materials couple and the bimetallic strips dimensions. The influence of the initial curvature δ_0 on the stability of a bimetallic strip is shown in figure 5a while figure 5b depicts the sensibility of the snapping temperature to the CTE difference and to the bimetallic strip's length.

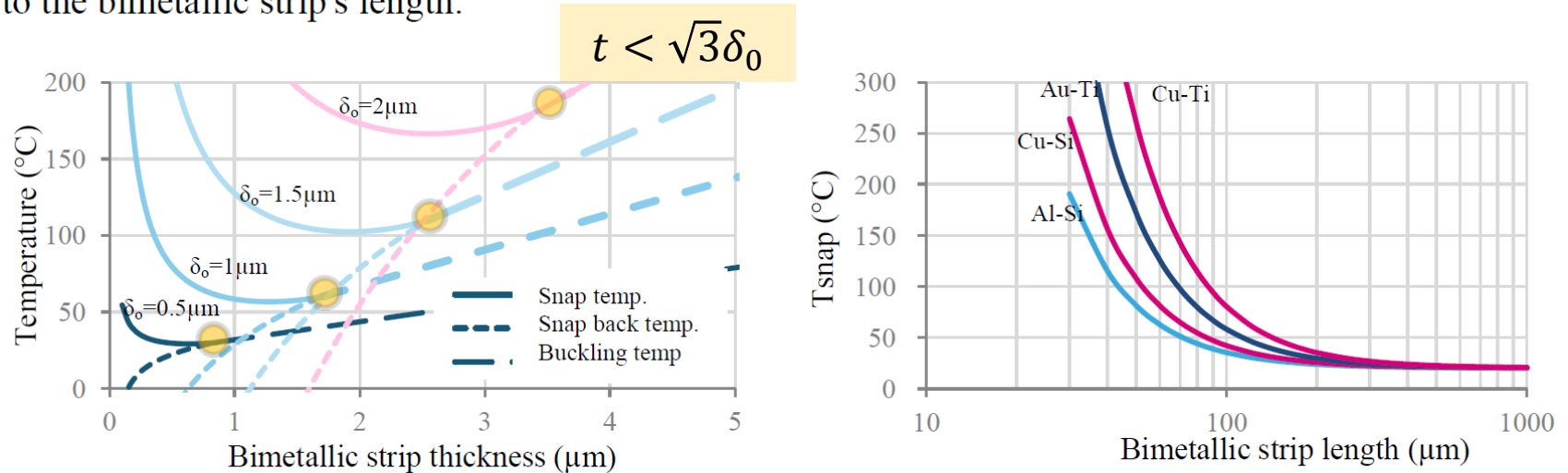


Figure 5. (a) Stability of Ti-Au bimetallic strips ($L=200\mu\text{m}$) as a function of the dimensions (thickness and middle deflection). (b) Snapping temperature (for $t = \delta_0\sqrt{3}=0.5\mu\text{m}$) as a function of the bimetallic strip length.

A. Arnaud, et al., J. Phys. Conf. Series 476 (2013) 012062

Commercially available b-TEH - prototype

TE-CORE /RF

ThermoHarvesting Wireless Sensor System

Featuring ThermoGenerator-in-Package TGP-651

Preliminary Datasheet

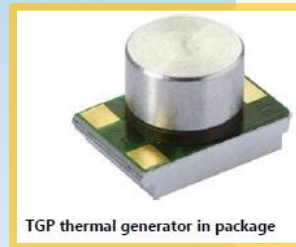
TE-CORE/RF is a fully functional and self-powered wireless sensor node, designed for evaluation and prototyping.

It measures and transmits temperature and voltage data in a 2/sec duty cycle for a virtually unlimited amount of time – **without batteries**.

All **power needed for its operation is harvested from excess or waste heat**. Heat **taken from the surface the device is mounted/magnetically attached to**. Thermoelectric conversion is done by a **single Micropelt TGP thermogenerator**.

Characteristics

- 2.4 V, **0.1 bis 10 mW thermoharvesting power** after DC Booster
- Detachable wireless sensor board
- 2.4 GHz, IEEE 802.15.4, Zigbee compliant
- Pre-qualified and certified RF module of IMST
- SPI, I²C, JTAG and configurable I/O interfaces
- User programmable

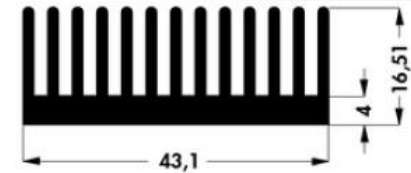


TGP thermal generator in package

TGP Properties

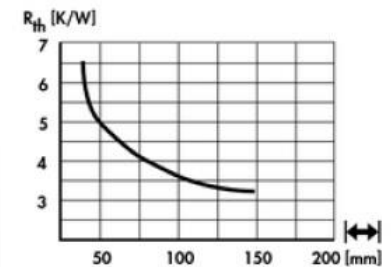


Different heat sink types of Sk422



Dimensions Sk422 heat sink

Properties of TGPs	TGP-65x
TEG chip inside	MPG-D655
Electrical resistance R_i	170 - 242 Ω
Thermal resistance R_{th}	28 K/W
Thermovoltage S	60 mV/K
Footprint (l x w x h)	15 x 10 x 9.3 mm



Performance diagram of Sk422 heat sink



*TGP-751 component is discontinued since Nov 2013

<http://www.micropelt.com/en/energy-harvesting/te-corerf.html>

Thank you for your attention!